Modified pendular vibration absorber for structures under base excitation

Pezo Eliot Z.[a] and Gonçalves Paulo B.[*]

Department of Civil Engineering, Pontifical Catholic University of Rio de Janeiro, PUC-Rio Rio de Janeiro, RJ, 22451-900, Brazil

Abstract.   The passive control of structures using a pendulum tuned mass damper has been extensively studied in the technical literature. As the frequency of the pendulum depends only on its length and the acceleration of gravity, to tune the frequency of the pendulum with that of the structure, the pendulum length is the only design variable. However, in many cases, the required length and the space necessary for its installation are not compatible with the design. In these cases, one can replace the classical pendulum by a virtual pendulum which consists of a mass moving over a curved surface, allowing thus for a greater flexibility in the absorber design, since the length of the pendulum becomes irrelevant and the shape of the curved surface can be optimized. A mathematical model for a building with a pendular tuned mass damper and a detailed parametric analysis is conducted to study the influence of this device on the nonlinear oscillations and stability of the main system under harmonic and seismic base excitation. In addition to the circular profiles, different curved surfaces with softening and hardening characteristics are analyzed. Also, the influence of impact on energy dissipation is considered. A detailed parametric analysis is presented showing that the proposed damper can not only reduce sharply the displacements, and consequently the internal forces in the main structure, but also the accelerations, increasing user comfort. A review of the relevant aspects is also presented.

Keywords: tuned mass damper; passive control; rolling pendulum; base motion; seismic excitation

1. Introduction

Passive control systems, due to their mechanical simplicity, have been used for many years to mitigate vibrations in civil engineering structures such as buildings, towers, bridges and industrial plants under the action of environmental forces such as wind and earthquakes and loads due to traffic and rotating machinery (Den Hartog 1956, Soong and Dargush 1997, Korenev and Reznikov 1993, Spencer and Nagarajaiah 2003). Among these systems, base isolation is considered to be the most appropriate system to improve the performance of structures during earthquakes (Kelly 1986, Villaverde 2009, Constantinou *et al.* 1998). However, the use of tuned mass dampers has been proposed as an efficient earthquake protective systems, especially when retrofitting existing structures, and designing high-performance structures such as hospitals and emergency response facilities (Kaynia *et al.* 1981, Pinkaew *et al.* 2003, Hoang *et al.* 2008, Matta 2011, Matta 2015).

The efficiency of the simultaneous use of base isolation and tuned mass damper has also been investigated (Petti *et al.* 2010, Xiang and Nishitani 2014).

Tuned mass dampers can enhance structural safety and integrity allowing protection of not only structural and non-structural elements but also building contents for considerably large earthquakes. Although the passive nature

can be seen as a limitation when compared to active and semi-active control systems, it is also a source of reliability since passive systems are not affected by discontinuous power supply during the seismic event and they have low maintenance requirements.

Pendulum mass dampers or pendulum vibration absorbers can be used as tuned mass dampers to suppress undesirable vibrations in several mechanical, civil and aerospace structures. The pendulum has usually a low frequency and uses gravity instead of elastic stiffness force. The passive control of structures using a pendulum tuned mass damper has been extensively studied in the technical literature and used in tall buildings such as the Taipei 101 in Taiwan (Kourakis 2007, Li *et al.* 2010) and the Crystal Tower in Osaka (Nagase and Hisatoku 1992), where earthquakes and strong typhoons are common occurrences. Nagase and Hisatoku (1992) presented some intrinsic features of a pendulum-type tuned-mass damper installed in a 37-story office building Crystal Tower in Osaka using the ice thermal storage tanks for air conditioning as the moving mass of the damper to reduce the lateral vibration of buildings. Ertas (1996) proposed a simple pendulum mounted to a tip mass of a beam as a vibration absorber. The autoparametric interaction between the first two modes of the system is investigated. Vyas and Bajaj (2001) studied the dynamics of autoparametric vibration absorbers using multiple pendulums. This problem was also tackled by Gus'kov *et al.* (2008) and Náprstek and Fischer (2009). Pinheiro (1997) studied analytically the classical non-linear pendulum connected to the structure by a rotational spring. Changes in the shape of the classical pendulum were also suggested by the author. Battista *et al.* (2003) investigated the structural response of transmission line towers under

---

[*]Corresponding author, Professor
  E-mail: paulo@puc-rio.br
[a]Ph.D.
  E-mail: eliotpz@hotmail.com

wind action and proposed the installation of non-linear pendulum-like dampers to reduce the along-wind displacements. Jankowski *et al.* (2004) analyzed the reduction of steel chimney vibrations with a pendulum damper. Gerges and Vickery (2005) derived the equations of motion for a translational single degree of freedom system equipped with a pendulum-type tuned mass damper. Through response minimization procedures, the optimum parameters of the TMD under random white noise excitations were determined. Lacarbonara and Ballerini (2009) proposed a passive vibration system to damp transverse vibrations of guyed masts, consisting of a number of pendula attached to the mast and tuned to the vibration modes to be controlled. By employing one pendulum only, tuned to the frequency of the lowest mode, the effectiveness of the passive system in reducing the motion and acceleration of the top section of the mast is demonstrated. Since detuning can sometimes lead to a significant loss of performance, Roffel *et al.* (2010) proposed a mechanical system to adjust the natural frequency and damping as an adaptive compensation for detuning in pendulum tuned mass dampers. Orlando and Gonçalves (2013) studied a hybrid system for vibration control of slender towers. The hybrid control is based on the simultaneous use of a pendulum absorber with an external force, dependent on the speed, on-off type, applied in the tower-pendulum connection, thus increasing the pendulum's efficiency in controlling vibrations. Finally, Fallahpasand *et al.* (2015) investigated the use of a nonlinear pendulum vibration absorber to control the resonance peak of a linear primary system and derived optimum damping and natural frequency ratios by minimizing the maximum steady-state response of the primary system.

Similar to a pendulum, a passive control system consisting of one or more spheres moving on a spherical surface at the top of the tower, creating a multidirectional damper, was studied by Chen and Georgakis (2013) to reduce the dynamic effects of wind on tall towers. A small-scale model was tested on a vibrating table. This system had previously been studied by Pirner (2002), who carried out theoretical and experimental studies and installed a TMD composed of a sphere inside a spherical vessel in a television tower in the Czech Republic.

As the frequency of the pendulum depends only on its length and the acceleration of gravity, to tune the frequency of the pendulum with that of the structure, the pendulum length is the only design variable. However, in many cases, the required length and the space required for its installation are not compatible with the project. In these cases, one can replace the classical pendulum by a virtual pendulum which consists of a mass moving over a curved surface, allowing thus for a greater flexibility in the absorber design, since the length of the pendulum becomes irrelevant and the shape of the curved surface can be optimized.

Analytical and experimental work for the understanding of the oscillatory motions of a body on different types of curved surfaces was carried out in the recent past. Shaw and Haddow (1992) developed several roller coaster experiments to model nonlinear oscillators with quadratic or cubic nonlinearity. Gottwald *et al.* (1992) developed
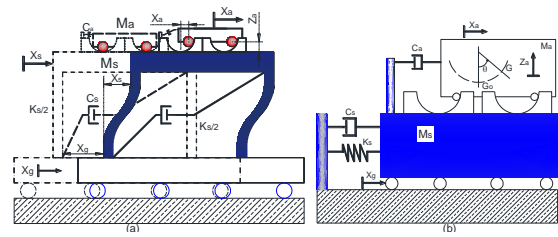

Fig. 1 Pendular tuned mass damper

analytical and experimental studies with the objective of studying the behavior of the Duffing equation through a rigid body that travels on a curved surface with two potential wells, simulating the Duffing equation with loss of stiffness. Further, Gottlieb (1997) derived the potential function of a curved surface on which a sphere moves by the influence of gravity in order to reproduce a linear or non-linear oscillator. Matta and De Stefano (2009a) studied, using a numerical simulation, how a tuned mass damper, commonly used in flexible structures under wind excitation, can be used in a building under seismic excitation. In this work they show schematically different types of pendular absorbers, some already studied in the literature. Subsequently Matta *et al.* (2009b) studied the use of a pendulum system in two directions for the seismic protection of buildings. Legeza (2013) proposed a pendulum damper consisting of a classic inverted pendulum where the mass moves on an isochronous curve.

Pendulum systems may present under severe loading conditions large amplitude oscillations, thus the linear assumption may lead to errors when oscillations become larger. The pendulum exhibits a softening behavior (Pasquetti and Gonçalves 2011) and may lead to various types of bifurcations and instabilities, as shown by Orlando and Gonçalves (2013). In order to limit the pendulum oscillations a pendular system with impact could be used, increasing the damping performance over a wide range of excitation frequencies and amplitudes (Bapat and Sankar 1985, Duncan *et al.* 2005). Collette (1998) studied numerically and experimentally the efficiency of a combined tuned absorber and pendulum impact damper to reduce the vibrations of a system under random excitation. The effectiveness of the optimal combined absorber and its sensitivity to variations of the clearance between the impact damper and tuned absorber, restitution coefficient and the mass ratio were analyzed.

The aim of the present work is to analyze the influence of a pendular tuned mass damper (PTMD) in the vibration control of structures, subjected to base motion, in particular harmonic and seismic loads. The pendular system consists of a mass that moves on a curved surface, generating forces similar to the classical pendulum. Several types of curve with hardening or softening characteristics are analyzed and compared with the circular case. This system has several advantages over existing systems such as ease of construction, returns naturally to the original position, have a small damping inherent to the system and easily enter in movement, leading to large reductions of displacements and accelerations. It should be noted that the technology for the construction of the pendulum system is well established; being the same used for the design of roller-coasters and

support devices for bridges and large structures, in particular roller bearings. To enhance the energy dissipations and/or prevent large pendulum oscillations the simultaneous use of a pendulum-impact system is also considered. The results show that the proposed damper can not only reduce sharply the displacements, and consequently the internal forces in the main structure, but also the accelerations, increasing user comfort.

2. Formulation of the PTMD

The main structure is modeled as a SDOF system with mass M_S, damping coefficient C_S, and lateral stiffness K_S, subjected to a time-dependent base displacement $X_g(t)$, where t is time. The horizontal displacement of the structure relative to the base is denoted by X_S. The pendular tuned mass damper proposed here, shown in Fig. 1, consists of a mass M_a that moves on a curved surface with constant or variable curvature, described by a function $Z_a(X_a(t))$, where Z_a and X_a are, respectively, the vertical and horizontal displacement components of M_a. C_a represents the viscous damping coefficient of the pendular device. The mass and inertia forces of the rollers are considered negligible. In addition, rolling without sliding is assumed in the trajectory direction, which is realistic for nearly all operation conditions (Pfeiffer *et al.* 2006). Also, the rolling friction in usually very small (Reynolds 1876), and the system may react swiftly to a short-term excitation. The number of wheels can be properly evaluated in order to distribute the weight of the mass M_a of the tuned mass damper, decreasing the contact force at each point. For a multi-story building, the values of M_S, C_S, and K_S can be taken, in a first approximation, as the modal mass, damping and stiffness relative to the first vibration mode (Soong and Dargush 1997).

This system generates nonlinear forces similar to those of the classical pendulum, but has the advantage of taking up little space, allowing simple variation of the radius of curvature, and, when destabilized, automatically return to the initial equilibrium position by the vertical component of the pendulum weight, which is not the case with many tuned mass dampers. Besides, being a smooth surface, it does not present discontinuities in the restoration forces, as it happens in sliding systems (stick-slip) and bases in the form of inclined planes.

The kinetic energy of the system is given as

$$T_s = \frac{1}{2}M_s\left(\dot{X}_g + \dot{X}_s\right)^2 + \frac{1}{2}M_a\left(\left(\dot{X}_g + \dot{X}_s + \dot{X}_a\right)^2 + \left(\frac{dZ_a}{X_a}\right)^2\left(\dot{X}_a\right)^2\right) \quad (1)$$

where the $\dot{X}_i = dX_i/dt$ denotes velocity (the overdot indicate differentiation with respect to time).

The total potential energy of the system is

$$\Pi = \frac{1}{2}K_s X_s^2 + M_a \cdot g \cdot Z_a \quad (2)$$

The Rayleigh function of the structure and pendular system, considering linear viscous damping, has the following form

$$R = \frac{1}{2}C_a\left(\left(\frac{dX_a}{d\theta}\dot{\theta}\right)^2 + \left(\frac{dZ_a}{d\theta}\dot{\theta}\right)^2\right) + \frac{1}{2}C_s\left(\dot{X}_s\right)^2 \quad (3)$$

By applying Hamilton's principle, the Euler-Lagrange equations of motion of the controlled structure are given by

$$\left(\ddot{X}_g + \ddot{X}_s\right)M_s + \left(\ddot{X}_g + \ddot{X}_s + \ddot{X}_a\right)M_a + C_s\dot{X}_s + K_s X_s = 0 \quad (4)$$

$$M_a\left(\ddot{X}_s + \ddot{X}_g\right) + M_a\left(\left(\frac{dZ_a}{dX_a}\right)^2 + 1\right)\ddot{X}_a +$$
$$M_a\left(\frac{dZ_a}{dX_a}\right)\left(\dot{X}_a\right)^2\frac{d^2Z_a}{dX_a^2} + M_a g\frac{dZ_a}{dX_a} + C_a\dot{X}_a\left(1 + \left(\frac{dZ_a}{dX_a}\right)^2\right) = 0 \quad (5)$$

Depending on the chosen function $Z_a(X_a(t))$, as observed in Eq. (5), inertial and geometric nonlinearities, as well as nonlinear damping forces, may appear in the equations of motion.

3. Circular surface

For a circular surface of constant radius of curvature R_c, the vertical and horizontal displacements of the mass can be written as a function of the rotation angle θ as (see Fig. 1(a))

$$X_a = R_c\sin(\theta) \text{ and } Z_a = R_c\left(1 - \cos(\theta)\right) \quad (6)$$

and the differential equations of motion (4) and (5) take the form

$$M_s\left(\ddot{X}_g + \ddot{X}_s\right) + M_a\begin{pmatrix}\ddot{X}_g + \ddot{X}_s + R\cos(\theta)\ddot{\theta} \\ -R\sin(\theta)\left(\dot{\theta}\right)^2\end{pmatrix} + C_s\dot{X}_s + K_s X_s = 0 \quad (7)$$

$$\begin{pmatrix}M_a\left(\cos(\theta)\ddot{X}_g + R\ddot{\theta} + g\sin(\theta) + \cos(\theta)\ddot{X}_s\right) \\ +C_a R\dot{\theta}\end{pmatrix}R = 0 \quad (8)$$

Introducing the following parameters

$$\omega_S^2 = \frac{K_S}{M_S}; \quad \frac{C_S}{M_S} = 2\xi_S\omega_S; \quad \frac{C_a}{C_S} = \delta\Delta\frac{\xi_a}{\xi_S}$$
$$\overline{X}_g = \frac{X_g}{R_c}; \quad \overline{X}_S = \frac{X_S}{R_c}; \quad \Delta = \frac{\omega_a}{\omega_S} = \frac{\sqrt{g}}{\omega_S\sqrt{R_c}};$$
$$\delta = \frac{M_a}{M_S}; \quad \tau = t\omega_S; \quad \frac{d\overline{X}_S}{d\tau} = \frac{1}{\omega_S}\frac{dX_S}{dt}; \quad (9)$$
$$\frac{d^2\overline{X}_S}{d\tau^2} = \frac{1}{\omega_S^2}\frac{d^2X_S}{dt^2}$$

where $\omega_a = \sqrt{g/R_c}$ is the characteristic frequency of a pendulum and ω_S is the frequency of the structure, Eqs. (10) and (11) is rewritten in the dimensionless form as

$$(\delta+1)\left(\frac{d^2\overline{X}_s}{d\tau^2}+\frac{d^2\overline{X}_g}{d\tau^2}\right)+\delta\cos(\theta)\frac{d^2\theta}{d\tau^2}+2\xi_s\frac{d\overline{X}_s}{d\tau}-$$
$$\delta\sin(\theta)\left(\frac{d\theta}{d\tau}\right)^2+\overline{X}_s=0 \tag{10}$$

$$\delta\cos(\theta)\left(\frac{d^2\overline{X}_s}{d\tau^2}+\frac{d^2\overline{X}_g}{d\tau^2}\right)+\delta\frac{d^2\theta}{d\tau^2}+2\delta\Delta\xi_a\frac{d\theta}{d\tau}+$$
$$\Delta^2\delta\sin(\theta)=0 \tag{11}$$

The equations of motion in dimensionless form, Eqs. (10) and (11), are a function of four parameters, damping ratios of the structure and PTMD, ξ_s and ξ_a, respectively, the mass ratio δ and ratio of natural frequencies, Δ. The main variable in terms of design of a TMD is the mass ratio, δ, which is taken usually as a small percentage of the mass of the structure. A conventional TMD of a few percent mass ratio yields the control effect via resonance, implying a fairly large movement relative to the primary structure. However, some authors (Matta and De Stefano 2009a, De Angelis *et al.* 2012) have advocated the use of large mass ratios for systems under base excitation, and a broad range of δ is considered in the present parametric analysis, to verify this hypothesis. Given the value of δ, the optimal values for ξ_s, ξ_a and Δ as a function of δ can be calculated.

4. Frequencies and vibration modes

From the linearization of Eqs. (12) and (13), the following eigenvalue problem is obtained

$$\begin{bmatrix} K_s-\lambda(M_a+M_s) & -\lambda R\cdot M_a \\ -\lambda M_a & M_a\cdot g-\lambda R\cdot M_a \end{bmatrix}\begin{Bmatrix} X_1 \\ X_2 \end{Bmatrix}=\begin{Bmatrix} 0 \\ 0 \end{Bmatrix} \tag{12}$$

where $\lambda=\omega_i^2$, and eigenvalues and eigenvectors represent respectively the natural frequencies and vibration modes of the system under analysis. The natural frequencies are given in dimensional form by

$$\omega_i=\frac{\sqrt{2}}{2}\sqrt{\frac{K_sR_c+M_ag+M_sg\mp\sqrt{\begin{array}{c}K_s^2R_c+2K_sR_cM_ag-2M_sR_cK_sg+\\M_a^2g^2+2M_aM_sg^2+M_s^2g^2\end{array}}}{M_sR_c}} \tag{13}$$

The two natural frequencies are a function of the mass and stiffness of the structure, acceleration of gravity and radius of curvature of the surface at the origin ($X_a=0$), which for a curved surface described by an arbitrary smooth continuous function $Z_a(X_a)$ is given by

$$R(X_a)=\left(1+\left(\frac{dZ_a}{dX_a}\right)^2\right)^{\frac{3}{2}}\left(\frac{d^2Z_a}{dX_a^2}\right)^{-1}\Bigg|_{X_a=0} \tag{14}$$

Considering the non-dimensional parameters (9), the natural frequencies are rewritten in dimensionless form as
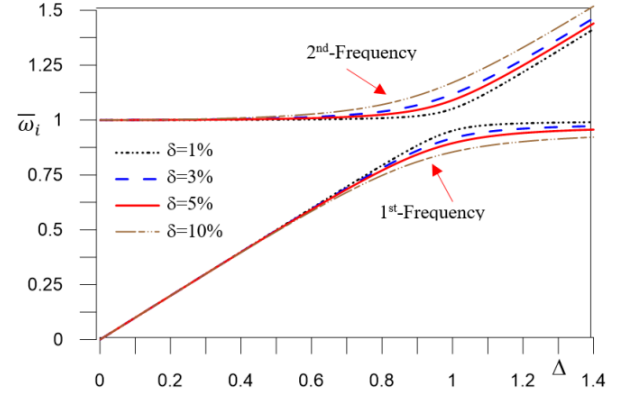

Fig. 2 Variation of the two dimensionless natural frequencies as a function of the dimensionless frequency ratio Δ for selected values of mass ratio δ

$$\overline{\omega}_i=\frac{1}{2}\sqrt{2\delta\Delta^2+2\Delta^2+2\mp2\sqrt{\delta^2\Delta^4+2\delta\Delta^4+\Delta^4+2\delta\Delta^2-2\Delta^2+1}};\quad i=1,2 \tag{15}$$

which depends on the mass and frequency ratios only.

Fig. 2 shows the variation of the two non-dimensional natural frequencies of the combined system (Eq. (15)) as a function of the frequency ratio Δ for selected values of the mass ratio, δ. For usual values of δ, the first frequency grows smoothly with Δ, from zero (radius of curvature infinite, flat surface), while the second non-dimensional frequency remains practically constant and equal to unity until it reaches the value $\Delta=1$, when the two normalized frequencies approach the unit value (ideal value for a classic TMD). From this point on, the two frequencies invert the behavior, with the second frequency growing in a practically linear fashion with Δ, while the first one tends to a constant value smaller than one.

The first vibration mode, considering a unit rotation for the PTMD, is given by $X_1=\left\{(\Delta^2-\overline{\omega}_1^2)\delta/(\delta\overline{\omega}_1^2),\ 1.0\right\}^T$. For a given value of δ, the first term of the eigenvector increases with Δ, as $\overline{\omega}_1$ increases (see Fig. 2). The structure moves in the same direction as the PTMD, in addition the mass of the PTMD has, for usual values of Δ, a displacement much greater than the mass of the structure, illustrating the energy transfer from the main system to the damper. The second vibration mode of the structure-PTMD system is given by $X_2=\left\{(\Delta^2-\overline{\omega}_2^2)\delta/(\delta\overline{\omega}_2^2),\ 1.0\right\}^T$. In this case the two masses move in opposite direction and the first term of the eigenvector decreases in magnitude with Δ.

5. Response under harmonic load

Initially the response of the building under a harmonic base motion is conducted. The parametric analysis is focused on two parameters: the mass ratio, varying within range $0.01\leq\delta\leq0.5$ and natural frequency ratio, within a range of $0.1\leq\Delta\leq1.3$. The damping ratio of the primary structure is taken into account by the representative value of $\xi_s=2\%$. The harmonic excitation is given in dimensionless

Table 1 Optimum values of the parameters Δ and ξ_S. (Warburton and Ayonride 1980)

Excitation	R_D	Δ_{opt}	ξ_{a-opt}
$Ae^{i\Omega t}$ Harmonic force	$\sqrt{1+\dfrac{2}{\delta}}$	$\dfrac{1}{1+\delta}$	$\sqrt{\dfrac{3\delta}{8(1+\delta)}}$
$\ddot{X}_g e^{i\Omega t}$ Harmonic base acceleration	$\sqrt{\dfrac{2}{\delta}(1+\delta)}$	$\dfrac{\sqrt{1-\dfrac{\delta}{2}}}{1+\delta}$	$\sqrt{\dfrac{3\delta}{8(1+\delta)\left(1-\dfrac{\delta}{2}\right)}}$
Random force	$\sqrt{\dfrac{1+\dfrac{3\delta}{4}}{\delta(1+\delta)}}$	$\dfrac{\sqrt{1+\dfrac{\delta}{2}}}{1+\delta}$	$\sqrt{\dfrac{\delta\left(1+\dfrac{3\delta}{4}\right)}{4(1+\delta)\left(1+\dfrac{\delta}{2}\right)}}$
Random base acceleration	$(1+\delta)^{3/2}\sqrt{\dfrac{1}{\delta}-\dfrac{1}{4}}$	$\dfrac{\sqrt{1-\dfrac{\delta}{2}}}{1+\delta}$	$\sqrt{\dfrac{\delta\left(1-\dfrac{\delta}{4}\right)}{4(1+\delta)\left(1-\dfrac{\delta}{2}\right)}}$

form by $d^2\overline{X}_g / d\tau^2 = 0{,}01\Delta^2\beta^2 sin(\beta\tau)$. The nonlinear equations of motion are numerically integrated using the fourth-order Runge-Kutta method.

Den Hartog (1956), considering an undamped structure, derived the following optimal parameters in terms of the mass ratio: $\Delta = 1/1+\delta$ and $\xi_a = \sqrt{3\delta/8(1+\delta)}$. Later Ayorinde and Warburton (1980) derived, analyzing several structural systems under different types of excitation, considering equivalent sdof models, the optimum values of the parameters Δ and ξ_S shown in Table 1 (Warburton 1982). These results can also be found in Soong and Dargush (1997), among others. Hoang *et al.* (2008) also derived optimal tuned mass damper parameters for seismic applications considering the effect of characteristic ground frequency and damping of primary structure. It is found that, in all cases, the optimal tuning frequency decreases and the optimal damping ratio increases as the mass ratio increases. They also show that considering damping in the primary structure lowers the optimal tuning frequency while, to a lesser degree, raises the optimal damping ratio of TMD for large mass ratios. Optimal parameters for several passive systems can be also found in Korenev and Reznikov (1993). Fig. 3 shows the variation of maximum normalized displacement of the controlled and uncontrolled response of the structure in the steady state regime as a function dimensionless excitation frequency parameter β (resonance curves), for three selected values of the mass ratio, using for the PTMD the optimal values presented in Table 1. Since the resonance curves of forced nonlinear systems may display points of dynamic bifurcation (saddle-node, pitchfork or period-multiplying bifurcations) and jumps, the resonances curves are obtained using numerical algorithms for the computation of bifurcation diagrams of the associated Poincaré map (Parker and Chua 1989, Orlando and Gonçalves 2013), with the dimensionless excitation frequency β as the control parameter.

A perceptible decrease in the vibration amplitudes in the resonance region is observed, showing that the PTMD is a reliable means to suppress undesirable vibrations of
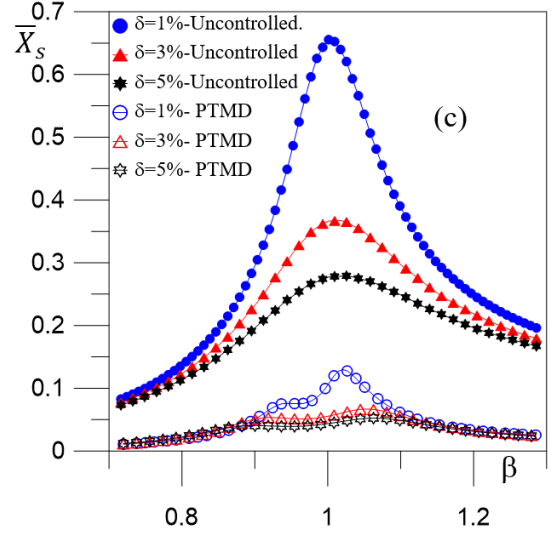
Fig. 3 Bifurcation diagram of the controlled and uncontrolled structure, for ξ_s=2%, and optimum values of ξ_a and Δ

Table 2 Maximum displacements and accelerations of the structure without and with PTMD for optimum values of ξ_a and Δ, under harmonic base excitation

Mass ratio δ	Structure with PTMD			Uncontrolled		Reduction (%)	
	Structure		PTMD				
	$\overline{X}_S$	$\ddot{\overline{X}}_S$	θ	$\overline{X}_S$	$\ddot{\overline{X}}_S$	$\overline{X}_S$	$\ddot{\overline{X}}_S$
1%	0.130	0.136	39.761	0.246	0.246	47.18	44.54
3%	0.067	0.095	14.807	0.234	0.234	71.48	59.54
5%	0.052	0.090	9.105	0.223	0.223	76.46	59.53

structures caused by harmonic base excitations. The difference between the curves of the uncontrolled system is due to the adimensionalization process where the non-dimensional displacement is divided by the optimal value of the radius of curvature R_c, which is a function of the optimal frequency ratio that is a function of $\boldsymbol{\delta}$ ($\Delta = \omega_a / \omega_S = \sqrt{g} / \omega_S \sqrt{R_c}$). The maximum displacements and accelerations of the structure under harmonic base excitation without and with PTMD for optimum values of ξ_a and Δ are shown in Table 2. As expected, the efficiency of the PTMD increases with $\boldsymbol{\delta}$, showing a reduction of 76,46% in the displacements and of 59,53% in the maximum acceleration for $\boldsymbol{\delta = 5}$%.

Observing the optimal values of the frequency ratio obtained by various authors, there is a definite trend for each value of β, with the tuning frequency decreasing with δ, followed by an increase in the damping ratio (see, for example, Table 1). So, in recent years researchers have proposed the use of TMDs with large mass ratio, comparable with the mass of the structure to be protected, to increase their seismic effectiveness (Matta and De Stefano 2009a, De Angelis *et al.* 2012). In order to avoid the introduction of an excessive additional weight, masses already present on the structure could be converted into tuned masses, retaining structural or architectural functions
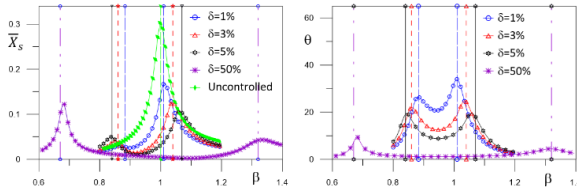
Fig. 4 Bifurcation diagrams of the structure and PTMD, for ξ_S=2%, ξ_a=3.5% and Δ=0.9

Table 3 Maximum displacements and accelerations of the structure and PTMD; for Δ=0.9 $\xi_s = 2\%$ and $\xi_s = 3.5\%$

Control		Mass ratio δ	Structure		PTMD
			$\overline{X}_S$	$\ddot{X}_S$	$\theta(°)$
PTMD Circular	A	1%	0.169	0.173	34.00
	B	3%	0.127	0.136	24.87
	C	5%	0.106	0.119	19.59
	D	50%	0.123	0.084	9.30
Uncontrolled	E		0.204	0.204	
Peak Reduction %	E-A		17.32	15.15	
	E-B		37.84	33.26	
	E-C		48.01	41.61	
	E-D		39.55	58.61	

(a) $\delta = 1\%$

(b) $\delta = 50\%$

Fig. 5 Reduction of the maximum steady-state displacements and accelerations as a function of Δ

beyond the mere control function. However, it must be pointed out that the optimal damping values are usually high (10.98% for $\delta = 5\%$) and the installation of additional dampers may be necessary to attain the optimal response. This is not effective in reducing the initial transient response of structures or when the structure is subjected to a short duration excitation.

Fig. 4 shows the variation of maximum displacement of the structure and maximum rotation angle of the PTMD during the steady state response as a function of the dimensionless excitation frequency β (resonance curves) for Δ=0.9, ξ_S=2% and ξ_a=3,5% considering four values of δ: 1%, 3%, 5% and 50%. The dashed vertical lines correspond to the two natural frequencies of the structure-PTMD system. For the correct interpretation of the results it is worth remembering that the dimensionless excitation force is dependent on β. Table 3 shows the maximum displacements and accelerations of the structure and rotation of the PTMD, as well as the reduction in the peak values when compared with the uncontrolled system. Comparing the results with those of the uncontrolled system and those of the controlled structure considering optimal parameters, even considering a small damping ratio for the PTMD, a robust decrease in the structural response is observed. The use of a large mass ratio ($\delta = 50\%$) is shown to be a reliable solution, decreasing not only the maximum displacement of the primary structure but also the PTMD rotations. Also, it is observed that the maximum displacement and rotations are almost zero in a broad range of the forcing frequency parameter β. Thus, the performance of the PTMD with a large mass ratio is not too
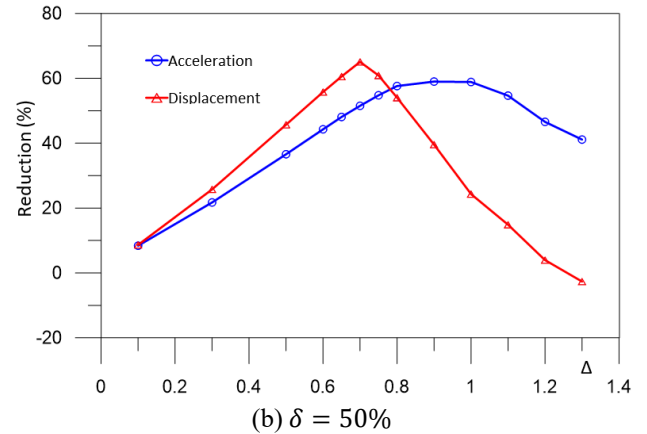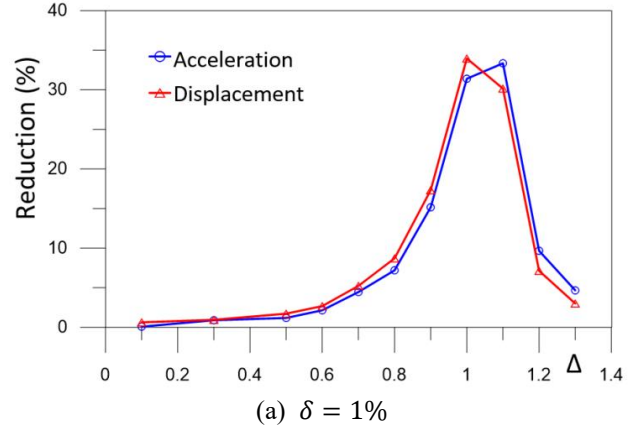
sensitive to uncertainty in the system parameters. On the other hand, for small values of δ the performance becomes more sensitive if its parameters shift away from the design values.

For the classical TMD the optimal values of frequency ratio are in the range $0.9 \leq \Delta \leq 1.0$. However the exact value of Δ is rather difficult to evaluate in a real structure or may vary due to deterioration, inadvertent changes to structure's properties and increased dead loads, which can lead to a significant loss of performance in tuned mass dampers. So, it is desirable to study the variation of the efficiency of the PTMD with Δ. Fig. 5(a) shows the reduction of the maximum displacement and acceleration of the structure with the frequency ratio, considering δ=1%, ξ_s=2% and ξ_a=3.5%. The PTMD can not only reduce the maximum displacement is a broad range of Δ, around the ideal value of Δ=1, increasing the safety of the structure, but also the maximum acceleration, increasing human comfort. Fig. 5(b) shows the results for δ=50%. These results, compared with those in Fig. 5(a), show that the PTMD with a large mass improves substantially the effectiveness of the damper, reducing considerably the displacements and accelerations in a much wider range of Δ, thus decreasing the sensitivity of the PTMD to the frequency ratio. This is particularly important for structures under seismic excitation where the frequency content of the signal is unknown a priori.

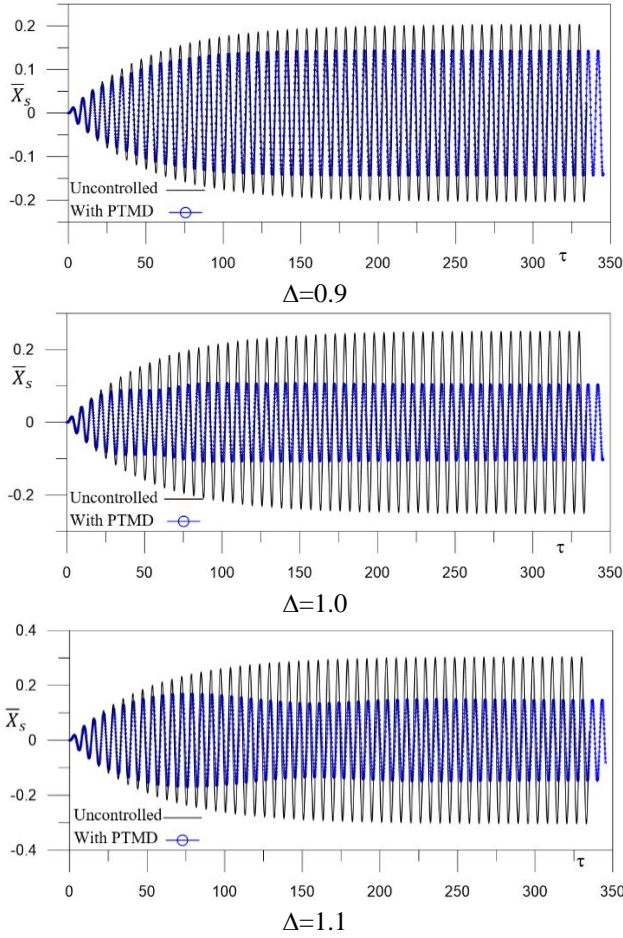Fig. 6 compare the time response of the uncontrolled

Fig. 6 Time response of the displacements of the uncontrolled and controlled structure at resonance. β=1.0; δ=0.01, ξ_s=2% and ξ_a=3.5%
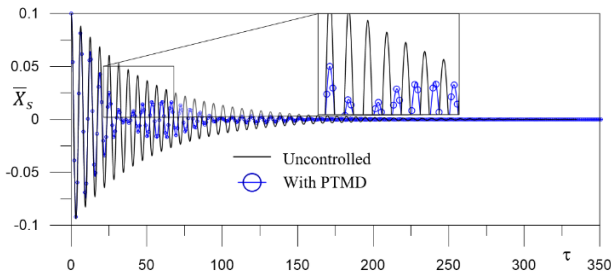

Fig. 7 Time response of the displacements of the uncontrolled and controlled structure subjected to an initial displacement (Xs=0.1) for δ=0.01, Δ=1.0 ξ_s =2% and ξ_a=3.5%
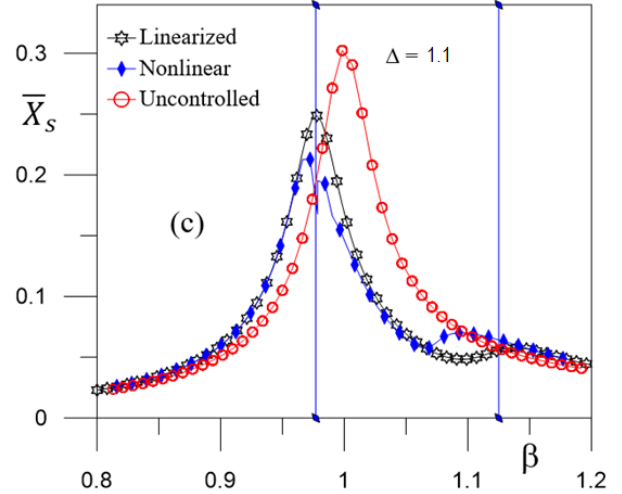

Fig. 8 Comparison of the structure uncontrolled, linearized and non-linearized responses; for ξ_s =2%, ξ_a =3.5%, δ=0.01, Δ=1.1 ξ_s=2% and ξ_a=3.5%

and controlled structure under harmonic base motion for three values of Δ (0.9, 1.0, 1.1), considering β=1.0 (resonance of the primary system) and δ=1%. Although the mass ratio is rather small, the beneficial effect of the PTMD is observed just after a few cycles decreasing the vibrations amplitudes in the steady-state and transient regimes. To test the effectiveness of the damper in the transient regime, Fig. 7 shows the time response of the uncontrolled and controlled structure subjected to an initial displacement ($\overline{X}_s$=0.1). As observed in the inset figure, just after a few

cycles the PTMD leads to a meaningful decrease in the displacements. Also, the energy dissipated by the mass damper is evident, with the structure converging swiftly to the static configuration, reducing the root-mean-square displacement response of the main structure.

As the rotation of the pendular system increases, the influence of its nonlinearity increases, as illustrated in Fig. 8 where the uncontrolled response is compared with the controlled response considering the non-linear and linearized equations of motion. The nonlinearity increases the efficiency of the control device reducing perceptibly the maximum displacement in the resonance region.

6. Response under seismic excitation

In practice, the earthquake excitation cannot be known a priori. Consequently a "true" optimal solution to control the structure under an unknown seismic excitation is impossible. Usually a base isolation system is preferable, but in many cases the installation of tuned mass dampers is a simple, effective, inexpensive, and reliable means to suppress undesirable vibrations. Under earthquake excitation, which is rather random, its performance, however, greatly depends on the characteristics of ground motion. Having this in mind, in the present analysis the N-S and E-W components of the El Centro earthquake and the E-W component of the Loma-Prieta earthquake are used to test the effectiveness of the PTMD. The maximum acceleration of the E-W Loma-Prieta accelerogram is 0.15 g, while the maximum acceleration of the N-S and E-W components of the El-Centro signal are, respectively, 0.35 g and 0.21 g (Lin *et al.* 2009). Fig. 9 show the power spectrum of these three signals as a function of β. Fig. 10 shows the time response of the displacements of the uncontrolled and controlled structure under seismic load (accelerogram of the EW component of the El Centro earthquake) for four selected values of the mass ratio δ(1%, 3%, 5%, 50%), considering in each case the optimal
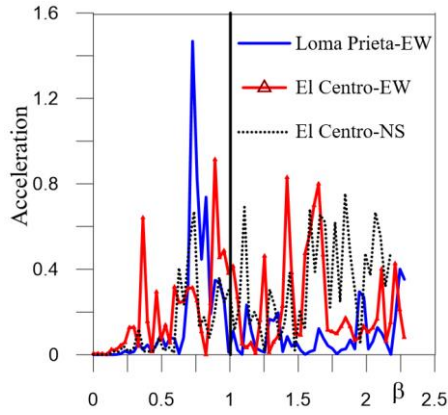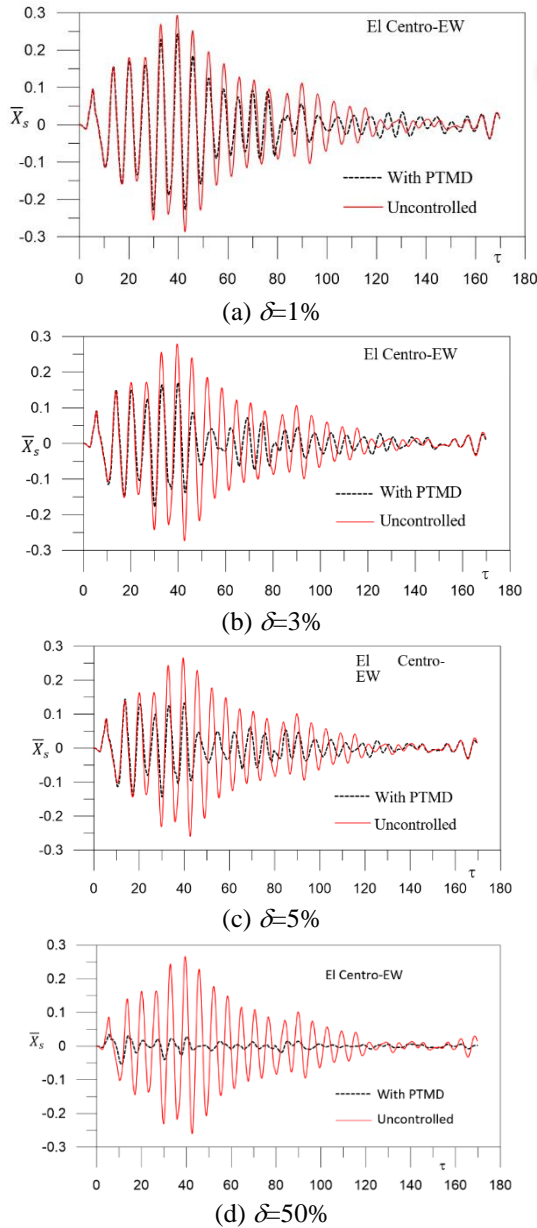
Fig. 9 Earthquake power spectrums in the region of interest

Table 4 Maximum displacements and accelerations of the structure and maximum rotations of the PTMD under seismic excitation as a function of Δ

Earthquake	Frequency ratio (Δ)	Structure-PTMD δ = 5%			Uncontrolled		Reduction (%)	
		Structure		PTMD				
		$(\overline{X}_s)$	$(\ddot{\overline{X}}_s)$	(θ^p)	$(\overline{X}_s)$	$(\ddot{\overline{X}}_s)$	$(\overline{X}_s)$	$(\ddot{\overline{X}}_s)$
Loma Prieta-EW	0.9	0.111	0.109	34.356	0.146	0.134	24.092	18.155
El Centro-EW		0.128	0.214	37.317	0.243	0.294	47.497	27.263
Loma Prieta-EW	1.0	0.143	0.139	28.127	0.181	0.165	20.608	15.935
El Centro-EW		0.168	0.247	48.708	0.300	0.363	44.072	32.135

Table 5 Maximum displacements and accelerations of the structure and maximum rotations of the PTMD under seismic excitation as a function of δ

9	Mass ratio (d)	Structure-PTMD-Δ = 0.9			Uncontrolled		Reduction (%)	
		Principal Structure		PTMD				
		$(\overline{X}_s)$	$\ddot{\overline{X}}_s$	(θ^p)	$\overline{X}_s$	$\ddot{\overline{X}}_s$	$\overline{X}_s$	$\ddot{\overline{X}}_s$
Loma Prieta-EW	0.01	0.128	0.12	44.226	0.146	0.134	12.299	10.527
El Centro-EW		0.205	0.273	52.892	0.243	0.294	15.927	7.254
Loma Prieta-EW	0.03	0.111	0.112	36.954	0.146	0.134	24.106	16.098
El Centro-EW		0.133	0.239	42.801	0.243	0.294	45.262	18.714
Loma Prieta-EW	0.05	0.111	0.109	34.356	0.146	0.134	24.092	18.155
El Centro-EW		0.128	0.214	37.317	0.243	0.294	47.497	27.263

(a) δ=1%

(b) δ=3%

(c) δ=5%

(d) δ=50%

Fig. 10 Time response of the displacements of the uncontrolled and controlled structure under seismic load (EW component of the El Centro) for three selected values of the mass ratio δ, considering in each case the optimal values of Δ and ξ_a. $\xi_s = 2$ %

values of Δ and ξ_a obtained by Warburton and Ayonride for random base acceleration (see Table 1) and $\xi_s = 2$ %. The beneficial effect of the PTMD on the response of the structure and its safety increases with the mass ration and the reduction in displacements occurs well before the uncontrolled structure reaches the maximum vibration amplitudes. For a large mass ratio, the PTMD becomes very effective in minimizing the primary structure response, increasing its safety under seismic excitation.

Table 4 shows the maximum displacements and accelerations of the controlled and uncontrolled structure and maximum rotations of the PTMD under seismic excitation for two values of Δ (0.9 and 1.0) and the reductions observed in the maximum displacements and accelerations in both cases considering the E-W components of the El Centro and Loma Prieta earthquakes, while Table 5 display the same comparison for three values of the mass ratio, δ. Here, $\xi_s = 2$ % and $\xi_s = 3.5$ %). In all cases a reduction of displacements is observed, but in some examples a small increase in accelerations occurs. There is a great variability in the reduction of displacements and accelerations due to the different frequency content of the three signals used and their magnitude. This shows the lower APMS efficiencies in the presence of random loads since their performance depends on a good tuning between the different frequencies existing in the earthquake signals and the APMS-structure system. The largest reduction in displacements was 47% for the El Centro-EW earthquake and Δ=0.9. The largest reduction in accelerations was 32%, also for the El Centro-EW earthquake, and Δ=1.0.

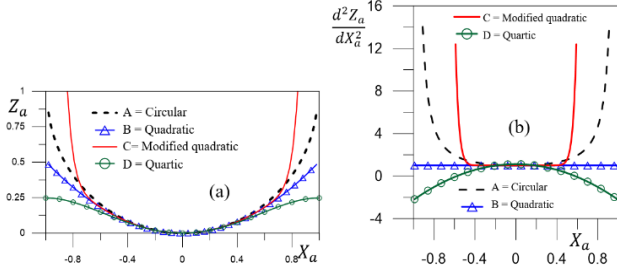Fig. 11 Functions describing the pendulum

Fig. 12 Bifurcation diagram of the: (a) Structure and (b) PTMD for the different types of curve (Δ=1.0)

7. Pendular device with variable radius

The radius of curvature of a curve described by any function $Z_a(X_a)$ is given by

$$R_c = \left(1+\left(\frac{dZ_a}{dX_a}\right)^2\right)^{\frac{3}{2}}\left(\frac{d^2Z_a}{dX_a^2}\right)^{-1} \quad (16)$$

To study the influence of the variable radius of curvature, three different types of surfaces defined below are used. Fist, a quadratic curve is considered

$$Z_a = X_a^2 / 4f \quad (17)$$

where f is the focal length. For comparison purposes, the radius of curvature at the origin ($X_a = 0$) is considered to be the same as that of the circular case, leading to $f=R_c/2$. Thus, a pendulum with increasing radius of curvature (length) is obtained, being given by

$$R(X_a) = R_c\left[1+\left(X_a/R_c\right)^2\right]^{3/2}.$$

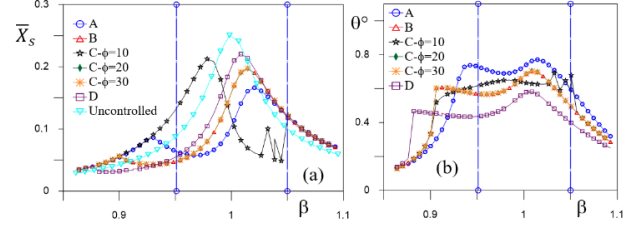The second curve to be analyzed is a quadratic curve modified by one exponential term of the form

$$Z_a = \frac{1}{4f}X_a^2 - bX_a^{2\phi}, \quad \text{with} \quad b = \frac{\left(-4mf^2+R_c^2\right)}{4fR_c^{2\phi}} \quad (18)$$

where m and ϕ are pre-defined geometric parameters used to increase the radius of curvature away from the origin (X_a=0), decreasing the displacement of the pendulum for large vibration amplitudes (nonlinear hardening behavior). Again, $f=R_c/2$. In both cases, a concave track is obtained.

The third curve to be analyzed is described by the following fourth order polynomial

$$Z_a = \frac{2h}{n^2}X_a^2 - \frac{h}{n^4}X_a^4 \quad (19)$$

with horizontal tangent line at X_a=0 and $X_a = \pm n$ and passing through the points $Z_a(\pm n)=h$. To have at the origin a radius of curvature equal to the circular track, $R_c=n^2/4h$. This polynomial is the potential energy of the softening nonlinear Duffing oscillator with negative cubic nonlinearity, having three equilibrium positions: X_a=0, which corresponds to a stable equilibrium position, a minimum, and X_a=$\pm n$ that are unstable equilibrium

Table 6 Maximum displacements and accelerations for each type of curve (δ=0.01; Δ=1.0)

Shape		Structure		PTMD
		$\overline{X}_s$	$\overline{\ddot{X}}_s$	$\overline{X}_s$
Uncontrolled	A	0.252	0.252	
Circular	B	0.166	0.173	0.771
Quadratic	C	0.197	0.203	0.703
M. Q.-ϕ=10	D	0.212	0.206	0.692
M. Q.-ϕ=20	E	0.197	0.202	0.705
M. Q. -ϕ=30	F	0.197	0.203	0.703
Quartic	G	0.220	0.223	0.582
	A-B	33.96	31.40	
	A-C	21.56	19.51	
Reduction (%)	A-D	15.62	18.21	
	A-E	21.73	19.68	
	A-F	21.56	19.51	
	A-G	12.51	11.22	

positions, two maxima.

The three curves are compared with the circular profile in Fig. 11. For the modified quadratic curve and the quartic curve the parameters m=800, ϕ=10, H=0.25 and n=1 are adopted. These surfaces are described in terms of the coordinates (X_a, Z_a). For the purposes of comparison with the circular curve, its equations are rewritten in term of X_a and Z_a, that is $Z_a = R_c - \sqrt{R_c^2 - X_a^2}$.

Fig. 12 shows the bifurcation diagrams of the Poincaré map for the PTMD described by five different types of curve and compare the results with those for the uncontrolled case considering δ=0,01, Δ=1, ξ_S=2% and ξ_a=3,5%. For the modified quadratic track (M.Q.), two additional values of ϕ are adopted, ϕ=20 and ϕ=30. Table 9 shows the maximum displacements and accelerations of the controlled and uncontrolled structure and maximum rotations of the PTMD. The resonance curves for the non-circular curves exhibit discontinuities. These jumps are due to the additional nonlinear terms in the equations of motion due to the variable radius of curvature (compare Eq. (5) with Eq. (8)). However, since in all cases smooth curves are adopted, no abrupt changes are observed in the system dynamics. This would occur if the track where described by different curves or inclined planes (Pfeiffer *et al*. 2006). The most efficient pendulum profile is the circular one leading to a reduction of 33.96% in the maximum displacements
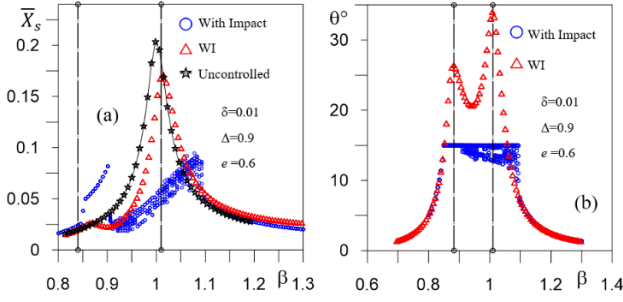
Fig. 13 Bifurcation diagram of: (a) structure and (b) PTMD with $\theta_{\lim}=15°$
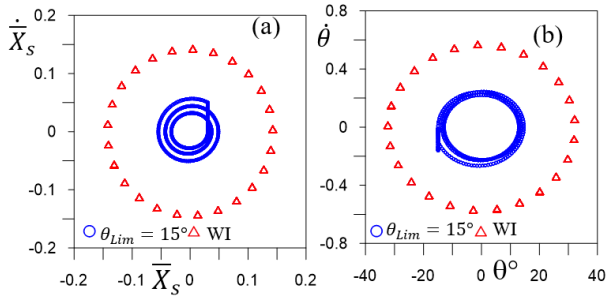

Fig. 14 Phase plane of: (a) structure, (b) PTMD with and without impact for $\beta=1.0$

and 31.40% in the maximum acceleration. The worst case is the quartic polynomial due to its softening characteristics (the curvature decreases as the vibration amplitude increases). The maximum displacement of the PTMD has in all cases the same order of magnitude. The variation of curvature leads to a pendulum with variable length. This is a highly nonlinear problem as shown by Belyakov *et al.* (2009) and Pasala and Nagarajaiah (2014). The oscillations of the PTMD in many cases, when its damping coefficient is small, may be large, but the technology for designing such systems is well known and has been used in the design of roller-coaster and other multibody systems (Tändl *et al.* 2007, Pombo and Ambrósio 2007, Pombo and Ambrósio 2003, Pfeiffer *et al*. 2006).

8. Impact system

As shown previously, the pendulum system can, in certain cases, display large rotations. Although this can be properly handled in the PTMD design, in certain circumstances this may be not desirable and barriers which limit its movement can be used, generating impact forces whose efficiency in vibration control is here briefly investigated. Consider that the maximum rotation permitted on the PTMD is controlled by two barriers located at a distance $\pm X_{máx}$ from the center of the surface. For the circular curve, the maximum horizontal displacement of the additional mass is thus defined in the dimensionless form as $\bar{X}_{\max}=\sin\left(\theta_{\lim}\right)$. The ratio of the final to initial velocity difference between the pendulum and the barrier after they collide is the coefficient of restitution, e, which normally ranges from 0 to 1 where 1 would be a perfectly elastic

collision and a perfectly inelastic collision has a coefficient of restitution 0. In order to handle the collision, an adaptive stepsize control for the Runge-Kutta algorithm is used. Thus, the nonlinear vibro-impact system with a nonzero offset barrier is now studied (Babitsky 2013). Fig. 13 shows, for $\delta=0.01$ and $\Delta=0.9$, a comparison of the response of the uncontrolled system with the response of the controlled system with and without impact, considering $\theta_{\lim}=15°$ and a coefficient of restitution $e=0.6$. A considerable decrease of the maximum displacements in the main resonance region due to impact is observed, when compared with the controlled response without impact. To illustrate this, Fig. 14 shows the phase plane of the steady-state response of the controlled system with and without impact, considering $\beta=1.0$, where the reduction in displacements and velocities due to impact is observed. The discontinuity in the velocity during impact brings about a strong additional nonlinearity, which leads to not only discontinuities in the resonance curve (jumps) but also to period-multiplying bifurcations. This problem will be analyzed in more detail in a future publication.

9. Conclusions

A pendular tuned mass damper (PTMD), consisting of a mass that moves on a curved track, was investigated in the present work. The dimensionless nonlinear equations of motion are derived for the model considering an arbitrary curved track and used in parametric analysis. The performance of the PTMD was investigated in a large parameter space including a broad range of forcing frequencies, mass ratios, tuning frequency ratio, damping ratios, track profile and impact characteristics. The results show that the PTMD is quite effective when the structure is subjected to a base harmonic excitation. It can not only reduce sharply the displacements, and consequently the internal forces in the main structure, but also the accelerations, increasing user comfort. Also, although more sensitive to the varying frequency content of known earthquake signals, the PTMD was shown to be also effective under seismic excitation. The optimal PTMD with large mass ratio with a lower tuning frequency and higher damping ratio was shown to be very effective in minimizing the primary structure response in a broad range of excitation frequency while generating fairly small displacements of the damper, being thus very robust with respect to detuning due to deviation in the structural properties and uncertainty in the system parameters. The effectiveness of a PTMD with large mass was observed both under harmonic excitation and seismic ground motion time histories with different frequency contents. The mass of non-structural components could in this case be used to achieve an appropriate mass ratio. The nonlinearity of the damper has a beneficial effect decreasing the displacements of the structure when compared to the linearized model of the pendulum. The considered non-circular tracks gives rises to nonlinear inertia, damping and geometric nonlinearities not present in the circular case, leading to jumps and bifurcations in the response of the PTMD and primary structures. Tracks with softening characteristics decrease

the efficiency of the damper. Finally, the results show that the PTMD with impact can adequately dissipate the translational energy of the main structure, increasing the effectiveness of the damper, being this dependent on the specific values of clearance and restitution coefficient. Multiple tuned mass dampers with distributed natural frequencies using the present configuration can be easily designed, as well as bi-directional dampers.

Acknowledgments

References

Ayorinde, E.O. and Warburton, G.B. (1980), "Minimizing structural vibrations with absorbers", *Earthq. Eng. Struct. Dyn.*, **8**(3), 219-236.

Babitsky, V.I. (2013), *Theory of Vibro-Impact Systems and Applications*, Springer Science & Business Media, Leicestershire, U.K.

Bapat, C.N. and Sankar, S. (1985), "Single unit impact damper in free and forced vibration", *J. Sound Vibr.*, **99**(1), 85-94.

Battista, R.C., Rodrigues, R.S. and Pfeil, M.S. (2003), "Dynamic behavior and stability of transmission line towers under wind forces", *J. Wind Eng. Industr. Aerodyn.*, **91**, 1051-1067.

Belyakov, A.O., Seyranian, A.P. and Luongo, A. (2009), "Dynamics of the pendulum with periodically varying length", *Phys. D: Nonlin. Phenom.*, **238**(16), 1589-1597.

Chen, J. and Georgakis, C.T. (2013), "Tuned rolling-ball dampers for vibration control in wind turbines", *J. Sound Vibr.*, **332**(21), 5271-5282.

Collette, F.S. (1998), "A combined tuned absorber and pendulum impact damper under random excitation", *J. Sound Vibr.*, **216**(2), 199-213.

Constantinou, M.C., Soong, T.T. and Dargush, G.F. (1998), *Passive Energy Dissipation Systems for Structural Design and Retrofit*, Multidisciplinary Center for Earthquake Engineering Research, New York, U.S.A.

De Angelis, M., Perno, S. and Reggio, A. (2012), "Dynamic response and optimal design of structures with large mass ratio TMD", *Earthq. Eng. Struct. Dyn.*, **41**, 41-60.

Den Hartog, J.P. (1956), *Mechanical Vibration*, McGraw-Hill, New York, U.S.A.

Duncan, M.R., Wassgren, C.R. and Krousgrill, C.M. (2005), "The damping performance of a single particle impact damper", *J. Sound Vibr.*, **286**(1), 123-144.

Ertas, A. (1996), "Pendulum as vibration absorber for flexible structures: Experiments and theory", *J. Vibr. Acoust.*, **118**, 559.

Fallahpasand, S., Dardel, M., Pashaei, M.H. and Mohammadi Daniali, H.R. (2015), "Investigation and optimization of nonlinear pendulum vibration absorber for horizontal vibration suppression of damped system", *Struct. Des. Tall Spec. Build.*, **24**, 873-893.

Gerges, R.R. and Vickery, B.J. (2005), "Optimum design of pendulum-type tuned mass dampers", *Struct. Des. Tall Spec. Build.*, **14**(4), 353-368.

Gottlieb, H.P.W. (1997), "Isodynamical tracks and potentials", *J. Sound Vibr.*, **199**(4), 667-678.

Gottwald, J.A., Virgin, L.N. and Dowell, E.H. (1992), "Experimental mimicry of Duffing's equation", *J. Sound Vibr.*, **158**(3), 447-467.

Gus'kov, A.M., Panovko, G.Y. and Van Bin, C. (2008), "Analysis of the dynamics of a pendulum vibration absorber", *J. Mach. Manufact. Reliab.*, **37**(4), 321-329.

Hoang, N., Fujino, Y. and Warnitchai, P. (2008), "Optimal tuned mass damper for seismic applications and practical design formulas", *Eng. Struct.*, **30**(3), 707-715.

Jankowski, R., Kujawa, M. and Szymczak, C. (2004), "Reduction of steel chimney vibrations with a pendulum damper", *Task Quarter.*, **8**(1), 71-78.

Kaynia, A.M., Biggs, J.M. and Veneziano, D. (1981), "Seismic effectiveness of tuned mass dampers", *J. Struct. Div.*, **107**(8), 1465-1484.

Kelly, J.M. (1986), "Aseismic base isolation: Review and bibliography", *Soil Dyn. Earthq. Eng.*, **5**(4), 202-216.

Korenev, B.G. and Reznikov, L.M. (1993), *Dynamic Vibration Absorbers*, Wiley & Sons, New York, U.S.A.

Kourakis, I. (2007), "Structural systems and tuned mass dampers of super-tall buildings: Case study of Taipei 101", Ph.D. Dissertation, Massachusetts Institute of Technology, Massachusetts, U.S.A.

Lacarbonara, W. and Ballerini, S. (2009), "Vibration mitigation of guyed masts via tuned pendulum dampers", *Struct. Eng. Mech.*, **32**(4), 517-529.

Legeza, V.P. (2013), "Efficiency of a vibroprotection system with an isochronous roller damper", *Mech. Sol.*, **48**(2), 168-177.

Li, Q.S., Zhi, L.H., Tuan, A.Y., Kao, C.S., Su, S.C. and Wu, C.F. (2010), "Dynamic behavior of Taipei 101 tower: Field measurement and numerical analysis", *J. Struct. Eng.*, **137**(1), 143-155.

Lin, J.L., Tsai, K.C. and Miranda, E. (2009), "Seismic history analysis of asymmetric buildings with soil-structure interaction", *J. Struct. Eng.*, **135**(2), 101-112.

Matta, E. (2011), "Performance of tuned mass dampers against near-field earthquakes", *Struct. Eng. Mech.*, **39**(5), 621-642.

Matta, E. (2015), "Seismic effectiveness of tuned mass dampers in a life-cycle cost perspective", *Earthq. Struct.*, **9**(1), 73-91.

Matta, E. and De Stefano, A. (2009b), "Seismic performance of pendulum and translational roof-garden TMDs", *Mech. Syst. Sign. Proc.*, **23**(3), 908-921.

Matta, E. and De Stefano, A. (2009a), "Robust design of mass-uncertain rolling-pendulum TMDs for the seismic protection of buildings", *Mech. Syst. Sign. Proc.*, **23**(1), 127-147.

Nagase, T. and Hisatoku. T. (1992), "Tuned pendulum mass damper installed in crystal tower", *Struct. Des. Tall Spec. Build.*, **1**(1), 35-56.

Náprstek, J. and Fischer, C. (2009), "Auto-parametric semi-trivial and post-critical response of a spherical pendulum damper", *Comput. Struct.*, **87**(19), 1204-1215.

Orlando, D. and Goncalves, P.B. (2013), "Hybrid nonlinear control of a tall tower with a pendulum absorber", *Struct. Eng. Mech.*, **46**(2), 153-177.

Parker, T.S. and Chua, L. (2012), *Practical Numerical Algorithms for Chaotic Systems*, Springer Science & Business Media.

Pasala, D.T.R. and Nagarajaiah, S. (2014), "Adaptive-length pendulum smart tuned mass damper using shape-memory-alloy wire for tuning period in real time", *Smart Struct. Syst.*, **13**(2), 203-217.

Pasquetti, E. and Gonçalves, P.B. (2011), "Application of Taylor expansions and symmetry concepts to oscillators with non-polynomial nonlinearities", *Int. J. Comput. Appl. Math.*, **6**(1), 57-70.

Petti, L., Giannattasio, G., De Iuliis, M. and Palazzo, B. (2010), "Small scale experimental testing to verify the effectiveness of the base isolation and tuned mass dampers combined control strategy", *Smart Struct. Syst.*, **6**(1), 57-72.

Pfeiffer, F., Foerg, M. and Ulbrich, H. (2006), "Numerical aspects of non-smooth multibody dynamics", *Comput. Meth. Appl.*

Mech. Eng., **195**(50), 6891-6908.

Pinheiro, M.A.S. (1997), "Non-linear pendulum absorber of lateral vibrations in slender towers", M.Sc. Dissertation, COPPE/UFRJ, Rio de Janeiro.

Pinkaew, T., Lukkunaprasit, P. and Chatupote, P. (2003), "Seismic effectiveness of tuned mass dampers for damage reduction of structures", *Eng. Struct.*, **25**(1), 39-46.

Pirner, M. (2002), "Actual behaviour of a ball vibration absorber", *J. Wind Eng. Industr. Aerodyn.*, **90**(8), 987-1005.

Pombo, J. and Ambrósio, J. (2007), "Modelling tracks for roller coaster dynamics", *Int. J. Vehicl. Des.*, **45**(4), 470-500.

Pombo, J. and Ambrósio, J.A. (2003), "General spatial curve joint for rail guided vehicles: Kinematics and dynamics", *Multib. Syst. Dyn.*, **9**(3), 237-264.

Reynolds, O. (1879), "On rolling-friction", *Philosophical Transactions of the Royal Society of London*, **166**, 155-174.

Roffel, A.J., Lourenco, R., Narasimhan, S. and Yarusevych, S. (2010), "Adaptive compensation for detuning in pendulum tuned mass dampers", *J. Struct. Eng.*, **137**(2), 242-251.

Shaw, S.W. and Haddow, A.G. (1992), "On 'roller-coaster' experiments for nonlinear oscillators", *Nonlin. Dyn.*, **3**(5), 375-384.

Soong, T.T. and Dargush, G.F. (1997*), Passive Energy Dissipation Systems in Structural Engineering*, Wiley, New York, U.S.A.

Spencer Jr, B.F. and Nagarajaiah, S. (2003), "State of the art of structural control", *J. Struct. Eng.*, **129**(7), 845-856.

Tändl, M., Kecskeméthy, A. and Schneider, M. (2007), "A design environment for industrial roller coasters", *Proceedings of the ECCOMAS Thematic Conference on Advances in Computational Multibody Dynamics*.

Villaverde, R. (2009), *Fundamental Concepts of Earthquake Engineering*, CRC Press Inc., New York, U.S.A.

Vyas, A. and Bajaj, A.K. (2001), "Dynamics of autoparametric vibration absorbers using multiple pendulums", *J. Sound Vibr.*, **246**(1), 115-135.

Warburton, G.B. (1982), "Optimum absorber parameters for various combinations of response and excitation parameters", *Earthq. Eng. Struct. Dyn.*, **10**(3), 381-401.

Xiang, P. and Nishitani, A. (2014), "Optimum design for more effective tuned mass damper system and its application to base-isolated buildings", *Struct. Contr. Health Monitor.*, **21**(1), 98-114.

CC